
Temporal trends of spatial correlation within the PM₁₀ time series of the AirBase ambient air quality database

Oliver Kracht*

European Commission – Joint Research Centre,
Institute for Environment and Sustainability, Air and Climate Unit,
Via E. Fermi 2749, I-21027 Ispra, Italy
Email: oliver.kracht@gmx.de
*Corresponding author

Florenzia Parravicini

Garageeks Ltd.,
31 Greenmount Office Park,
Harolds Cross Bridge, Dublin 6w, Ireland
Email: parravicini.florenzia@gmail.com

Michel Gerboles

European Commission – Joint Research Centre,
Institute for Environment and Sustainability, Air and Climate Unit,
Via E. Fermi 2749, I-21027 Ispra, Italy
Email: michel.gerboles@jrc.ec.europa.eu

Abstract: We analyse the temporal variations which can be observed within time series of variogram parameters (nugget, sill and range) of daily air quality data (PM₁₀) over a ten years time frame. Datasets have been obtained from previous geostatistical analysis of country wide datasets from the AirBase ambient air quality database. Applying the Kolmogorov-Zurbenko filtering method, the time series are first decomposed into their short-, mid-, and long-term components. Based on this, we then evaluate the magnitude of the individual spectral signal contributions. Furthermore, the significance of a long term trend component is investigated by a block-bootstrap-based approach combined with linear regression. It is discussed if within these datasets the times series of nugget variance can provide information about the evolution of the measurement uncertainty of the related air pollutant, whereas the sill and the range parameters could contain information about the spatial representativeness of the monitoring stations.

Keywords: air pollution; air quality monitoring; measurements; uncertainty; geostatistics; spatial correlation; variogram; time series; model validation.

Reference to this paper should be made as follows: Kracht, O., Parravicini, F. and Gerboles, M. (2015) 'Temporal trends of spatial correlation within the PM₁₀ time series of the AirBase ambient air quality database', *Int. J. Environment and Pollution*, Vol. 58, Nos. 1/2, pp.63–78.

Biographical notes: Oliver Kracht has been a Postdoctoral Researcher at the European Commission Joint Research Centre in Ispra (Italy) since 2012, where he has been working on geostatistical methods for the evaluation of ambient air quality data. He graduated from the Department of Geosciences at the University of Bochum (Germany). Following an employment at the University of Lausanne (Switzerland), he moved to the Swiss Federal Institute of Aquatic Science and Technology. In 2007, he obtained his PhD in Environmental Engineering from the ETH Zurich. He worked as a PostDoc at the University of Bern (Switzerland), and as a Marie Curie Fellow at the Geological Survey of Norway.

Florencia Parravicini holds a BSc in Life Sciences from the University of Pau and Pays de l'Adour, France, and an MSc in Environmental Sciences from the University of Insubria, Italy. She has worked at the European Commission Joint Research Centre in Ispra (Italy) during years 2011 and 2012 and contributed to the scientific research project 'Geostatistics in Air Quality Assessment'. She is currently developing an electronic prototype for air quality monitoring by using simple, low-cost and mobile sensors connected to an Arduino open-source hardware device.

Michel Gerboles graduated in Analytical Chemistry from the University of Bordeaux (FR). In 1990, he joined the Joint Research Centre of the European Commission, as quality officer of the European Reference Laboratory for Air Pollution. His activities range from the improved calibration of primary reference methods for air quality monitoring to the organisation of proficiency testing and intercomparison exercises in support to the European policy on air quality. His current research interests include the validation of novel inexpensive gas sensor technologies, and the development of automatic methods for the extraction of quality indicators from large ambient air monitoring datasets.

This paper is a revised and expanded version of a paper entitled 'Trends of daily variogram parameters derived by geostatistical analysis of PM₁₀ time series from the AirBase ambient air quality database' presented at the 16th International Conference on Harmonisation within Atmospheric Dispersion Modelling for Regulatory Purposes, Varna, Bulgaria, 8–11 September 2014.

1 Introduction

A common step in the evaluation of model performance and in model validation is to compare the modelled results to observations obtained from air quality monitoring. In this context, statistical indicators which aim to determine whether model results have reached a sufficient level of agreement with the observations, require an estimate or an assumption to be made for both the measurement uncertainties and the spatial representativeness of the air quality parameters being used. Quantitative values for the measurement uncertainty are usually derived from experimental work specifically addressing the individual measurement techniques. Quantification of spatial representativeness in conventional practice is frequently based on the evaluation of specific site characteristics and assumptions being made about similarities of those characteristics within the surrounding domains. However, in order to facilitate the thorough exploitation of comprehensive observation datasets, the use of geostatistical

techniques can serve as an interesting alternative which can immediately be applied to the monitoring data without need to refer to secondary information. The underlying idea is that within such datasets the nugget variance can provide information about the measurement uncertainty and the micro-scale variability of the related air quality measurements, whereas the sill and the range parameter contain information about their spatial representativeness [for a more detailed introduction to this conceptualisation please refer to Gerboles and Reuter (2010)]. However, this information is assumed to be obfuscated by several atmospheric processes which are superimposing the signal of interest on a range of different time scales.

2 Geostatistical techniques

Geostatistics is a branch of applied statistics that quantifies the spatial dependence and the spatial structure of a measured property. It is based on the regionalised variable theory by which spatial correlation of measured properties can be treated (Matheron, 1963). Commonly, geostatistical analysis expresses the spatial correlation structure of the observations of an environmental variable x (e.g., a pollutant concentration) in terms of the variogram (sometimes also called the semivariogram). For this purpose the experimental semivariance $\gamma(l)$ is calculated to

$$\gamma(l) = \frac{1}{2} \frac{1}{n(l)} \sum_{i=1}^{n-1} [z(x_{i+l}) - z(x_i)]^2 \quad (1)$$

where $n(l)$ is the number of sample pairs at each lag distance l , and $z(x_i)$ and $z(x_{i+l})$ are the values of x at the locations i and $i + l$. It is usual to fit the experimental semivariance values with a simple continuous model function in which the semi-variance γ is described as a function of lag distance l (the theoretical variogram). In this context the Gaussian, the exponential or the spherical variogram models are the most commonly used. The spherical model [equation (2)] is often considered the best choice when spatial autocorrelation decreases to a point after which it becomes zero.

$$\begin{aligned} \gamma(l) &= C_0 + C_1 \left[1.5 \frac{l}{a} - 0.5 \left(\frac{l}{a} \right)^3 \right] & \text{if } 0 \leq l \leq a \\ \gamma(l) &= C_0 + C_1 & \text{if } l > a \end{aligned} \quad (2)$$

The parameters of the spherical model consist of the nugget C_0 , the partial sill C_1 , and the range a . The nugget variance C_0 represents the variability of the observations at small distances (tending towards 0). The empirical nugget variance is unknown since it is the value of the theoretical variogram at the origin. The nugget parameter C_0 is thus estimated by extrapolating the variogram towards $l = 0$. From this point, the semivariance increases until the full sill variance $C_0 + C_1$ is reached at a lag distance called the range (a). The range provides the distance beyond which semivariances remain constant. Up to this distance, observations of the regionalised variable in the sampling locations are correlated, afterwards they must be considered to be spatially independent. Note specifically that the term *partial sill* (shorthand *pSill*) is used to denote C_1 , whereas the term *sill* denotes $C_0 + C_1$.

3 Material and methods

In this study, we analysed the temporal variations observed within time series of variogram parameters obtained from different country wide datasets of daily average PM₁₀ data from the AirBase v.4 ambient air quality database. For the scope of this exercise, it was decided to apply the evaluation to the sole stations of background type, but for all area types (urban, suburban and rural). The assessment extends over a ten years time frame (1997 to 2007) and considers data from six different countries (FR, DE, GB, AT, IT and NL). The original material comprising comprehensive variogram parameter sets with time series of nugget (C_0), partial sill (C_1), and range (a) had already been established from variogram model fits within earlier projects (Gerboles et al., 2016). In this primary work a spherical variogram model had been used. More details about these previously reported analyses and about the underlying geostatistical computations can be obtained from Gerboles and Reuter (2010) and from Kracht et al. (2014). An overview about the number of variogram fits available within the ten years time frame is given in Table 1.

Table 1 Overview of available variography sets (individual variogram models fitted to PM₁₀ daily values), and summary of median values obtained for the nugget, partial sill and range parameter

Country	Available variogram fits				Summary of median values		
	First available [year]	Last available [year]	Available fits [count]	Accepted fits [count]	Nugget (2s) [$\mu\text{g}/\text{m}^3$]	pSill (2s) [$\mu\text{g}/\text{m}^3$]	Range [deg]
FR	2001	2007	2,051	1,221	6.45	9.17	0.50
DE	1998	2007	3,232	1,555	6.99	9.25	0.82
GB	1997	2007	3,932	2,415	6.13	7.01	0.34
AT	2001	2007	2,280	1,189	8.29	11.31	0.66
IT	2003	2007	1,737	890	12.67	19.85	0.85
NL	2003	2007	1,258	1,235	7.97	8.29	-

Notes: Note that nugget and partial sill values have been converted from spatial variances to standard deviations times two (2s) and are thus presented in units of [$\mu\text{g}/\text{m}^3$].

Constraints applied for accepting a valid variogram model fit have been:

- (I) $1 < \text{Nugget} < 150 (\mu\text{g}/\text{m}^3)^2$
- (II) $0 < \text{pSill} < 10^4 (\mu\text{g}/\text{m}^3)^2$
- (III) $0.01 < \text{Range} < 2 \text{ deg}$
- (IV) $0.04 < \text{pSill}/\text{Nugget} < 5 \cdot 10^3$

All simulation codes used in this study were developed in the R environment (R Development Core Team, 2014). In order to extend the necessary capacities, we included functionalities from the packages ‘kza’ (Close and Zurbenko, 2013), ‘boot’ (Canty and Ripley, 2013; Davison and Hinkley, 1997), and ‘Kendall’ (McLeod, 2011).

In a first step, the time series of variography parameters were screened for internal consistency by applying a set of constraints (I, II, III, IV, see note in Table 1) for accepting a valid variogram model fit (Table 1).

In a second preparatory step, the nugget and partial sill values of the accepted model fits were converted from spatial variances to spatial standard deviations times two

[equation (3)]. This transformation was preferred for the convenience of the later discussion (e.g. a comparison of nugget values to the uncertainty of measurements derived from independent laboratory studies or field exploration studies). Note that nugget and partial sill are thus presented in units of $\mu\text{g}/\text{m}^3$ and that the shorthand '2s' is used to indicate that parameters have been transformed in this manner. Range values remain untransformed and are expressed in units of spherical degrees.

$$\begin{aligned} \text{Nugget}(2s) &= 2\sqrt{C_0} \\ \text{pSill}(2s) &= 2\sqrt{C_1} \end{aligned} \quad (3)$$

Using the Kolmogorov-Zurbenko (KZ) filtering method (Rao et al., 1997; Eskridge et al., 1997) we then aimed to separate the original time series $X(t)$ into its different components [equation (4)].

$$X(t) = e(t) + S(t) + W(t) \quad (4)$$

In this conceptualisation, the short-term component $W(t)$ is attributable to variations of weather and to short-term fluctuations in precursor emissions. The mid-term (seasonal) component $S(t)$ can be interpreted as a result of changes in the solar angle (induced variations of emissions and temperature dependencies). The long-term signal $e(t)$ can be interpreted to result from long-term changes in overall emissions, pollutant transport, climate, economics, and environmental policies (Wise and Comrie, 2005). $e(t)$ is as well supposed to be influenced by evolutions in the operational principles of the monitoring network. In addition, $\text{Baseline}(t)$ is defined as the sum of the long-term and seasonal component. For the decomposition of the raw data time series, a KZ filter with $k = 5$ iterations of a moving average window of $m = 15$ days ($\text{KZ}[15,5]$) was used for extracting the baseline. A $\text{KZ}[365,3]$ filter was used to obtain the long-term signal $e(t)$. Note that $\text{KZ}[15,5]$ has a low pass periodicity of 34 days, while $\text{KZ}[365,3]$ has a low pass periodicity of 632 days.

Finally, the significances of long term trend components of the nugget and the sill and range effect were investigated from the slope of linear regression lines fitted to each set of the unfiltered time series $X(t)$. This required specific care to be taken because of the serial autocorrelation inherent in these data, which became evident from systematic patterns observed in $S(t)$. A simple linear regression would have all observations within an individual time series of variogram parameter values assumed to be independent. This is likely to give reasonable estimates of the regression coefficients, but to overstate their significance. To obtain more accurate confidence intervals, we chose to combine linear regression with a block-bootstrap-based approach (Künsch, 1989). In this way, the slope parameter was estimated by ordinary linear regression applied to bootstrap replicates chosen randomly from the original time series. We used a variable block length following a geometric distribution with a mean value of 30 days (CF-Interval 1) and 365 days (CF-Interval 2), respectively. Confidence intervals on the 95% level were then estimated by applying a coverage factor of 1.96 to the empirical standard deviation of the bootstrapped slope estimates. After some initial tests, it was considered suitable to perform 10,000 resamplings per time series to obtain good stability in the significance level estimates.

4 Results and discussion

Figures 1, 2 and 3 are illustrating the decomposition and trend analysis being applied to the nugget, partial sill and range time series of background stations from six different countries (FR, DE, GB, AT, IT and NL). In addition, an overview of the medians calculated for the raw parameter values of nugget, partial sill and range is given in Table 1. Note that for convenience of discussion nugget and partial sill values have been converted from variances to standard deviations times two and are thus presented in units of $\mu\text{g}/\text{m}^3$.

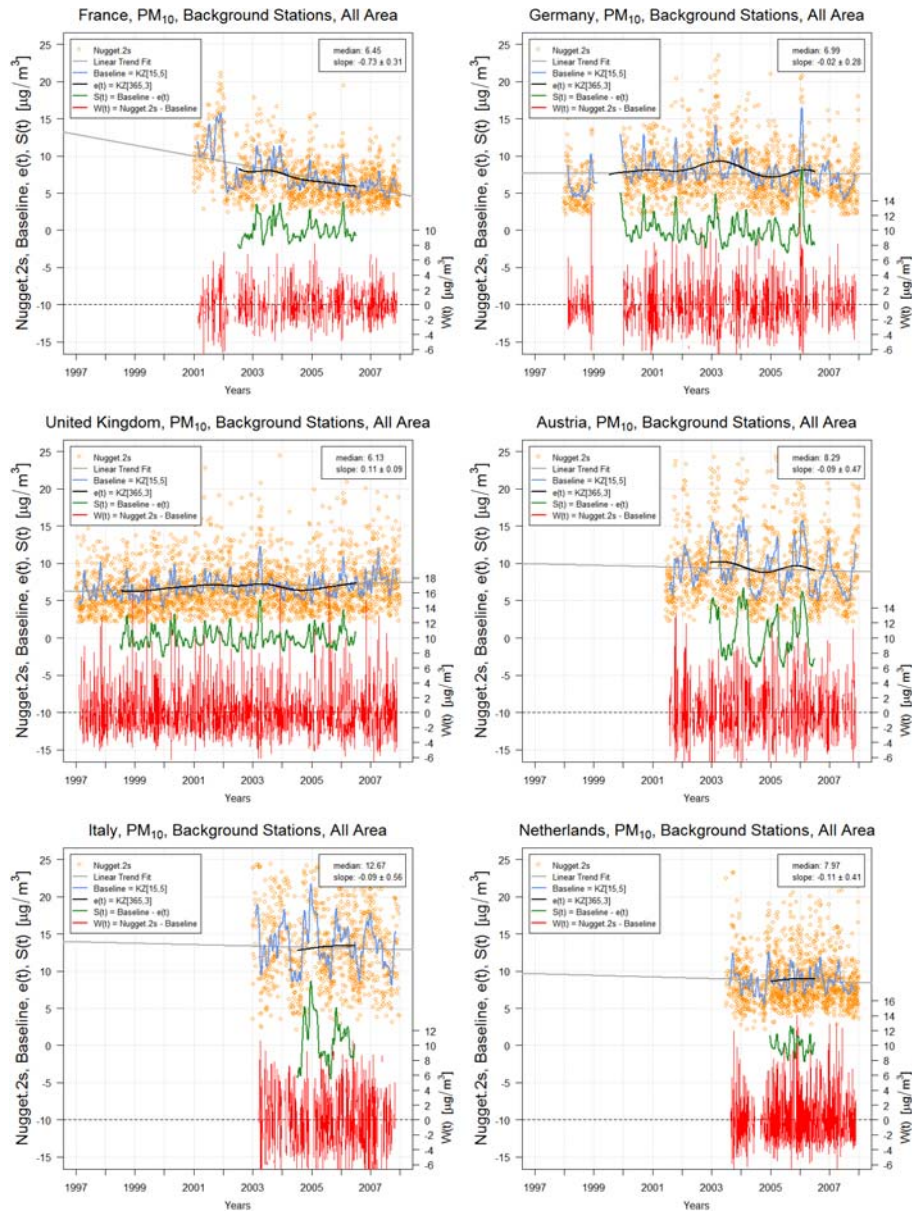
As a first observation from the aggregated absolute values of spatial variation (Table 1), both the nugget and the partial sill are highest for Austria and Italy. This general characteristic is indicating limitations in the spatial continuity of the data. It appears obvious that this effect could be due to the stronger topographic roughness and dissection of these two countries. However, other possible causes could be considered, like the impact of different sub-networks which might work independently and potentially according to non-synchronised procedures, or the impact of the variety of monitoring equipments and/or calibration techniques being used.

In contrast to these observations made for the nugget and partial sill, considering the aggregated values from the whole time series, a similarly generalisable observation cannot be made for the range parameter. This is actually because for some of the countries a clear interpretation of the range parameter is complicated by a superimposed trend component, as will be discussed later.

A closer look at the time series (Figures 1, 2 and 3) reveals that several data series are showing a pronounced cyclic behaviour in their seasonal component $S(t)$, and a non-stationarity (change of variance over time) in their short-term component $W(t)$. These effects clearly indicate the presence of temporal variations in the macroscale spatial correlation structures (partial sill and range). Furthermore, for the examples of Austria, Italy, Germany and France, a distinct phase relationship of the $S(t)$ component consisting in a winter increase of the sill effect is observed. It is likely that spatial variability increases in winter time because of local emission caused by heating, sanding and particulate matter re-suspension, as well as by limited air mixing increasing the discontinuity of PM_{10} concentration levels. However, for Austria and Italy this phase relationship is also observed in the nugget effect time series, which might indicate the influence of increasing small scale variability in winter time, too. Notably, in contrary to the abovementioned observations made for the nugget and partial sill, a clear phase relationship cannot be identified in the $S(t)$ component of the range time series.

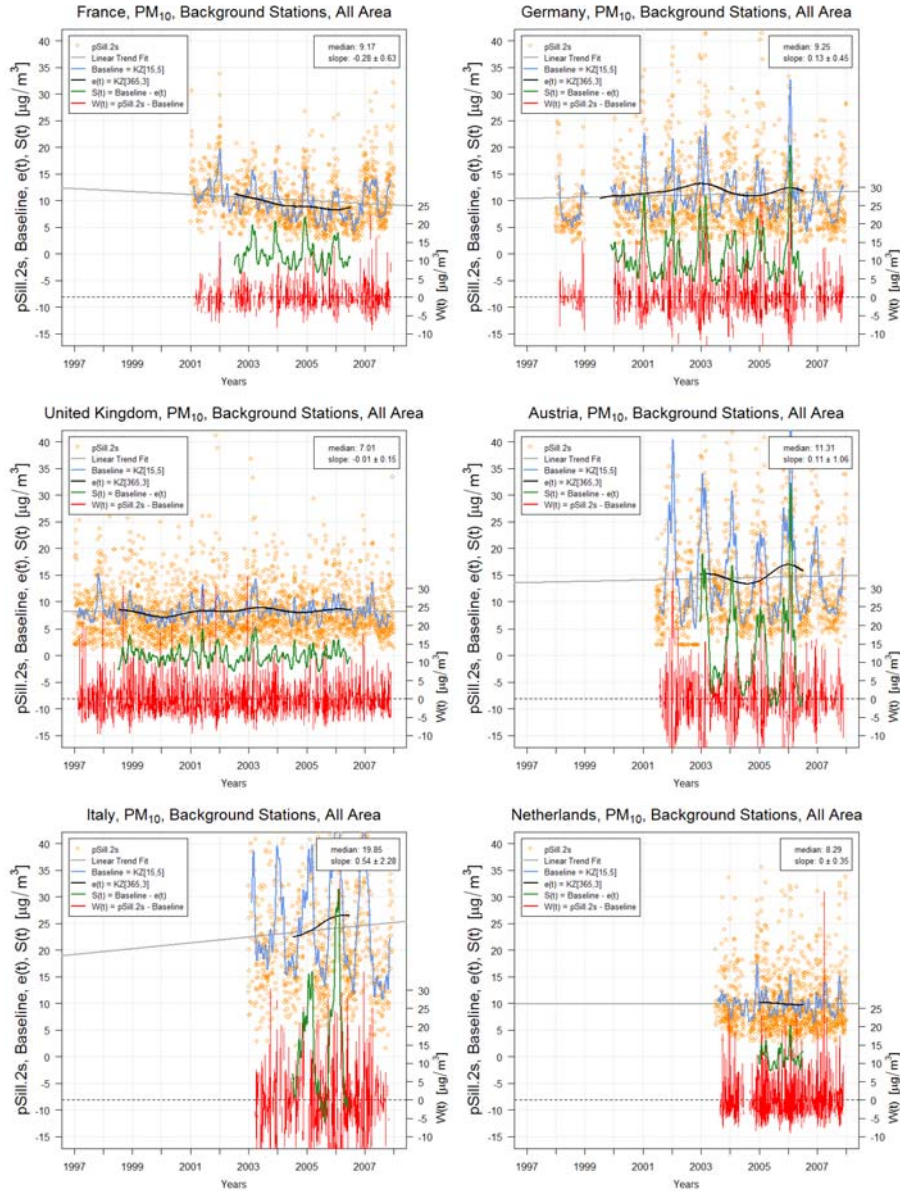
Exploring in more detail the nugget effect time series is indeed of high practical interest, as it can provide information about the evolution of the average measurement uncertainty of the related air pollutant (in this context average measurement uncertainty refers to a characterisation across a country dataset, as opposed to the individual measurement uncertainty of a single station). From a conceptual point of view, the two dominant causes for the nugget effect do consist of the uncertainty of the measurements and of the microscale variability (i.e. variations at distances smaller than the sampling distance). For the generalised case it is actually difficult to distinguish the proportions contributed by these two components, by using information obtained from geostatistics and time series analysis only. However, in order to account for these difficulties and to minimise the influence of small scale variability the datasets used in this exercise have already been preselected to comprise background type stations only.

Figure 1 Time series of estimated nugget parameter values from spherical variogram models fitted to PM₁₀ daily values of AirBase v.4 background stations (see online version for colours)



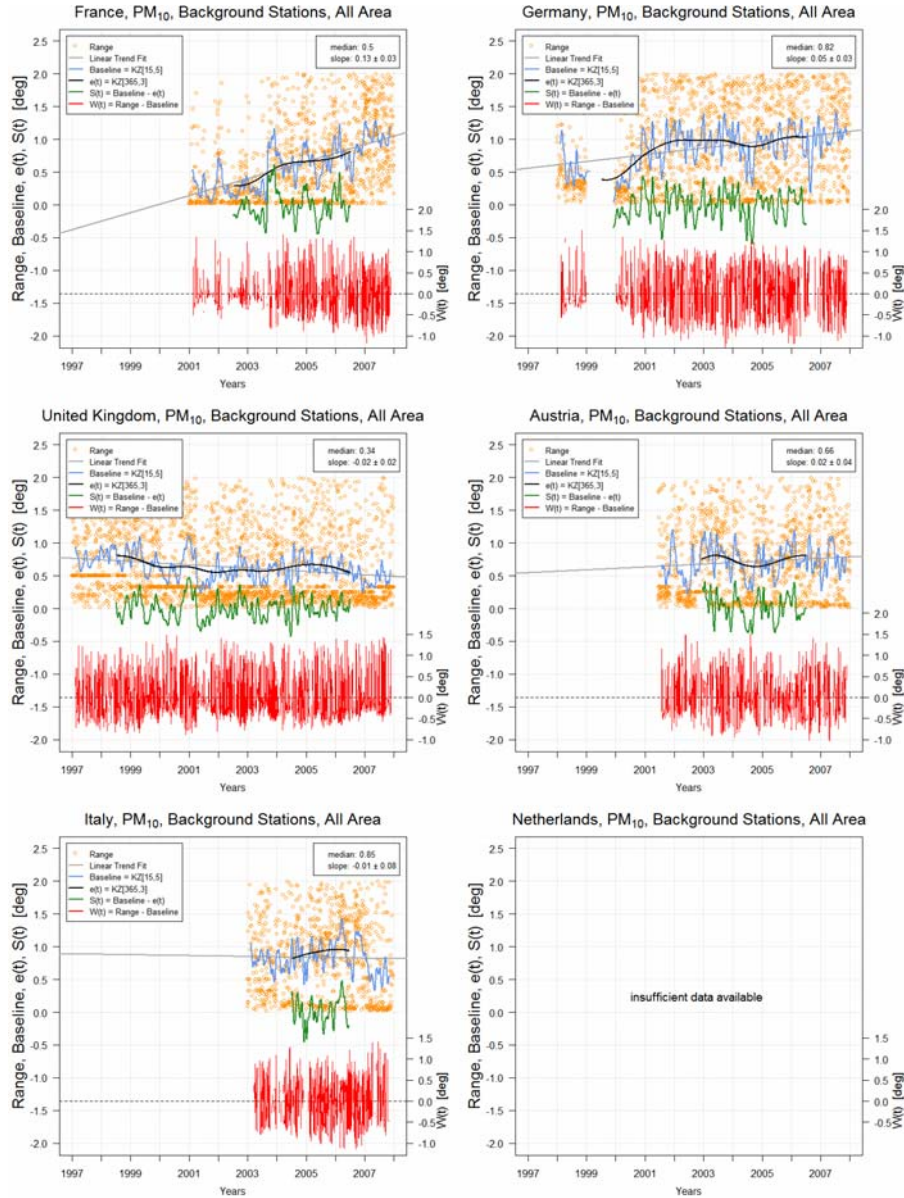
Notes: Nugget values have been converted from spatial variances to spatial standard deviations times two (2s) and are in units of $\mu\text{g}/\text{m}^3$. The KZ[15,5] filter has a low pass periodicity of 34 days that gives the baseline air quality. KZ[365,3] has a low pass periodicity of 632 days. $W(t)$ can be used to characterise the short-term component, $S(t)$ for the seasonal component, and $e(t)$ reflects the long-term signal and trend. $\text{Baseline}(t)$ is defined as the sum of the long-term and seasonal component.

Figure 2 Time series of estimated partial sill parameter values from spherical variogram models fitted to PM₁₀ daily values of AirBase v.4 background stations (see online version for colours)



Notes: Partial sill values have been converted from spatial variances to spatial standard deviations times two (2s) and are in units of $[\mu\text{g}/\text{m}^3]$. The $KZ[15,5]$ filter has a low pass periodicity of 34 days that gives the baseline air quality. $KZ[365,3]$ has a low pass periodicity of 632 days. $W(t)$ can be used to characterise the short-term component, $S(t)$ for the seasonal component, and $e(t)$ reflects the long-term signal and trend. $Baseline(t)$ is defined as the sum of the long-term and seasonal component.

Figure 3 Time series of estimated range parameter values from spherical variogram models fitted to PM_{10} daily values of AirBase v.4 background stations. Range values are presented in units of geographical coordinates [deg] (see online version for colours)



Notes: Data for the Netherlands have been omitted, because of convergence problems observed with the variogram fitting algorithm applied to this country (singularities due to a correlation between the sill and range estimates in this specific dataset). The $KZ[15,5]$ filter has a low pass periodicity of 34 days that gives the baseline air quality. $KZ[365,3]$ has a low pass periodicity of 632 days. $W(t)$ can be used to characterise the short-term component, $S(t)$ for the seasonal component, and $e(t)$ reflects the long-term signal and trend. $\text{Baseline}(t)$ is defined as the sum of the long-term and seasonal component.

Interpretations of seasonal effects on the spatial correlation lengths and on the small scale variability of the actual PM_{10} concentrations have been discussed in the previous paragraph. Nevertheless, the observed short term influences (non-stationarities) and seasonal variations in the nugget time series are equally well compatible with the assumption of related short term influences and seasonal fluctuations of the measurement uncertainty. Indeed, as the composition and properties of particulate matter and ambient parameters (like temperature and relative humidity) vary in time, they do as well influence the uncertainty of the different PM_{10} mass measurements principles (Pernigotti et al., 2013).

The magnitudes of the individual spectral signal contributions to the temporal variation of the nugget, partial sill and range parameter time series can be compared from the overall variance calculated for each of the filter-separated time series. Table 2 provides an overview of the observed temporal variances. In addition, Table 3 summarises normalised values, for which the total values of the four filter-separated spectral components have been adjusted by division with the total variance of the corresponding raw values. Example given for interpretation, the seasonal component $S(t)$ is strongly pronounced within the data series of Austria and Italy (absolute values in Table 2). Also the short term component $W(t)$ has its largest expression in the datasets of these latter two countries. In analogy to the interpretation of the median parameters of the total spatial variation (Table 1), we consider that this observation once more indicates a lack of spatial continuity of PM_{10} most likely due to the stronger topographic roughness and dissection as compared to the other countries. However, as discussed before with regard to the evaluation in the time domain, an influence by the effects of different PM_{10} measurements principles cannot be finally ruled out.

Table 2 Overall temporal variance of the raw variogram parameter estimates and of the filtered time series

Country	Parameter	Raw values [$(\mu\text{g}/\text{m}^3)^2$]	Baseline [$(\mu\text{g}/\text{m}^3)^2$]	$e(t)$ [$(\mu\text{g}/\text{m}^3)^2$]	$S(t)$ [$(\mu\text{g}/\text{m}^3)^2$]	$W(t)$ [$(\mu\text{g}/\text{m}^3)^2$]
FR	Nugget (2s)	2.51	1.48	0.14	0.46	1.16
DE	Nugget (2s)	3.28	0.94	0.08	0.73	1.96
GB	Nugget (2s)	2.87	0.43	0.03	0.34	2.16
AT	Nugget (2s)	5.41	1.95	0.06	2.28	3.17
IT	Nugget (2s)	6.50	2.09	0.01	2.34	4.28
NL	Nugget (2s)	2.92	0.47	0.00	0.30	2.21
FR	pSill (2s)	5.98	1.99	0.19	1.33	2.76
DE	pSill (2s)	13.95	3.86	0.14	4.00	7.32
GB	pSill (2s)	6.50	0.73	0.05	0.57	5.04
AT	pSill (2s)	30.47	15.29	0.34	16.44	13.58
IT	pSill (2s)	53.66	26.47	0.54	29.76	26.16
NL	pSill (2s)	8.38	0.94	0.01	0.74	6.63

Notes: The time series have not been de-trended for these calculations. Note that because nugget and partial sill values have been converted from spatial variances to standard deviations times two (2s), the unit for the temporal variance of the time series is $(\mu\text{g}/\text{m}^3)^2$.

Table 2 Overall temporal variance of the raw variogram parameter estimates and of the filtered time series (continued)

Country	Parameter	Raw values [deg ²]	Baseline [deg ²]	$e(t)$ [deg ²]	$S(t)$ [deg ²]	$W(t)$ [deg ²]
FR	Range	0.58	0.33	0.16	0.21	0.47
DE	Range	0.63	0.30	0.20	0.21	0.55
GB	Range	0.53	0.19	0.06	0.16	0.48
AT	Range	0.56	0.23	0.06	0.20	0.49
IT	Range	0.57	0.22	0.04	0.20	0.51
NL	Range	-	-	-	-	-

Notes: The time series have not been de-trended for these calculations. Note that because nugget and partial sill values have been converted from spatial variances to standard deviations times two (2s), the unit for the temporal variance of the time series is ($\mu\text{g}/\text{m}^3$)².

Table 3 Normalised temporal variance of the raw variogram parameter estimates and of the filtered time series

Country	Parameter	Raw values [normalised]	Baseline [normalised]	$e(t)$ [normalised]	$S(t)$ [normalised]	$W(t)$ [normalised]
FR	Nugget (2s)	1	0.59	0.06	0.18	0.46
DE	Nugget (2s)	1	0.29	0.02	0.22	0.60
GB	Nugget (2s)	1	0.15	0.01	0.12	0.75
AT	Nugget (2s)	1	0.36	0.01	0.42	0.59
IT	Nugget (2s)	1	0.32	0.00	0.36	0.66
NL	Nugget (2s)	1	0.16	0.00	0.10	0.75
FR	pSill (2s)	1	0.33	0.03	0.22	0.46
DE	pSill (2s)	1	0.28	0.01	0.29	0.52
GB	pSill (2s)	1	0.11	0.01	0.09	0.78
AT	pSill (2s)	1	0.50	0.01	0.54	0.45
IT	pSill (2s)	1	0.49	0.01	0.55	0.49
NL	pSill (2s)	1	0.11	0.00	0.09	0.79
FR	Range	1	0.57	0.28	0.36	0.81
DE	Range	1	0.48	0.32	0.33	0.87
GB	Range	1	0.36	0.11	0.30	0.91
AT	Range	1	0.41	0.11	0.36	0.88
IT	Range	1	0.39	0.07	0.35	0.89
NL	Range	-	-	-	-	-

Notes: For this table, all temporal variances have been normalised by the temporal variance of the raw values. Note that the time series have not been de-trended for these calculations.

In contrast to these observations made for Austria and Italy, Great Britain and the Netherlands are characterised by the lowest absolute seasonal variation $S(t)$ of the nugget

and the partial sill parameter (Table 2). On the other hand, because of this weakly pronounced $S(t)$ component, the relative importance of $W(t)$ is most prominent for these two countries (normalised values in Table 3). Finally, for the range parameter, results from Tables 2 and 3 suggest that the magnitudes of signal contributions from the seasonal and short term components ($S(t)$ and $W(t)$) are more homogeneously distributed across the different countries. However, the range parameters of France and Germany reveal a significant trend signal $e(t)$, as will be discussed in more detail later.

Results of the trend analysis are presented in Table 4. A significant trend component could only be found in the nugget time series of France (a negative slope of $-0.73 \pm 0.31 \mu\text{g}/\text{m}^3/\text{year}$) and Great Britain (a slightly positive slope of $0.11 \pm 0.09 \mu\text{g}/\text{m}^3/\text{year}$), and in the range time series of France (a positive slope of $0.13 \pm 0.03 \text{ deg}/\text{year}$) and Germany (a positive slope of $0.05 \pm 0.03 \text{ deg}/\text{year}$). For all other series the slope of the linear trend component was not significant in consideration of the bootstrapped confidence intervals. As an important note, the expressiveness of the trend analyses was somewhat limited by the relatively short extend of the valid variogram time series for some of the countries.

Table 4 Summary of the bootstrap-based trend analyses performed on the nugget, partial sill and range parameter time series

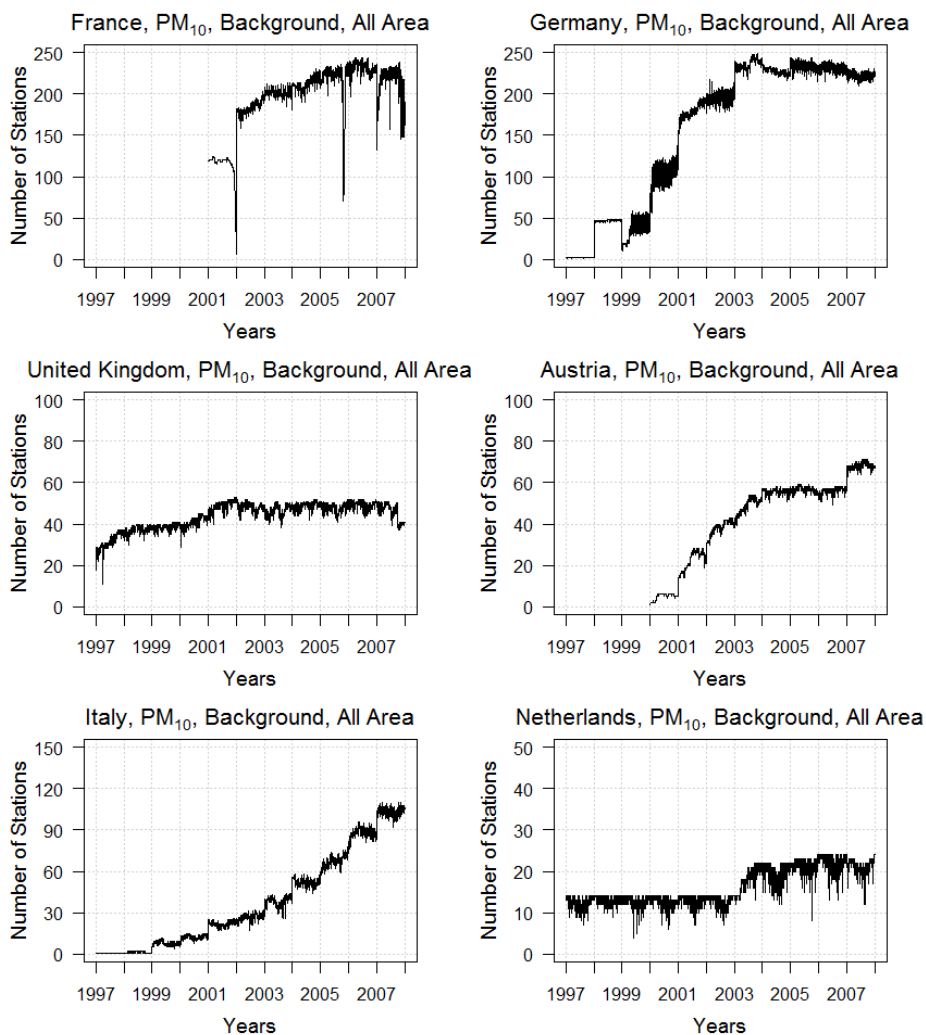
Country	Parameter	Trend slope [$\mu\text{g}/\text{m}^3/\text{year}$]	95% Conf-Int-1 [$\mu\text{g}/\text{m}^3/\text{year}$]	95% Conf-Int-2 [$\mu\text{g}/\text{m}^3/\text{year}$]	Significant?
FR	Nugget (2s)	-0.73	± 0.24	± 0.31	Yes
DE	Nugget (2s)	-0.02	± 0.18	± 0.28	No
GB	Nugget (2s)	0.11	± 0.07	± 0.09	Yes
AT	Nugget (2s)	-0.09	± 0.41	± 0.47	No
IT	Nugget (2s)	-0.09	± 0.51	± 0.56	No
NL	Nugget (2s)	-0.11	± 0.30	± 0.41	No
FR	pSill (2s)	-0.28	± 0.44	± 0.63	No
DE	pSill (2s)	0.13	± 0.36	± 0.45	No
GB	pSill (2s)	-0.01	± 0.11	± 0.15	No
AT	pSill (2s)	0.11	± 1.04	± 1.06	No
IT	pSill (2s)	0.54	± 1.89	± 2.28	No
NL	pSill (2s)	0.00	± 0.45	± 0.35	No
		[deg/year]	[deg/year]	[deg/year]	
FR	Range	0.13	± 0.02	± 0.03	Yes
DE	Range	0.05	± 0.02	± 0.03	Yes
GB	Range	-0.02	± 0.01	± 0.02	No
AT	Range	0.02	± 0.03	± 0.04	No
IT	Range	-0.01	± 0.05	± 0.08	No
NL	Range	-	-	-	-

Notes: The 95% confidence intervals Conf-Int-1 and Conf-Int-2 are corresponding to a resampling with mean block lengths of 30 days and 365 days respectively.

A negative trend in the nugget time series can be interpreted by an improvement of the measurement uncertainty of the monitoring stations over the years, but also by a

reduction in small scale variability (change in the nature or quantity of emissions, transported pollution, or atmospheric reactions). Other reasons causing either negative or positive trends might be the increase/decrease of the number of monitoring stations or a change in the station classifications. A positive trend in the range time series indicates that measurements of stations are becoming more homogeneous. This can be caused by an increase of quality actions performed on the measuring stations over the years. However, as for the nugget time series, a trend of the range values might also be the result of a change in the nature or quantity of emissions, pollution transport, or atmospheric reactions, as well as it could result from an increase/decrease of the number of monitoring stations or from a change in the station classifications.

Figure 4 Time series of the number of stations available for the analysis



Note: Note that if less than 20 stations were available at a given time step (i.e. day), the semi-variogram analysis was not performed.

In a final analysis, we counterchecked to which extent the trend analysis could have been affected by factors related to temporal fluctuations in data availability. Figure 4 provides time series of the number of stations available for the geostatistical analysis per day. As a general observation, the amount of monitoring stations available increases over time. This has a direct influence on the feasibility of the variogram parameter estimation. In fact the algorithm used in Gerboles and Reuter (2010) constrained the geostatistical analysis to those days with a minimum number of 20 stations being available. Example given, it is for this reason that the variogram analysis for the Netherlands dataset was not feasible for time sections before ca summer 2003. On the other hand, nearly all Netherland data fulfilling this constrained subsequently delivered a valid variogram model fit, which can be explained by the prevailing spatial continuity of PM_{10} data for this country.

Within a given network the number of monitoring stations is directly linked with the distribution of distances between these stations. Against this background, the nugget parameter C_0 needs to be considered as being an extrapolated value. Consequently, the accuracy of its estimation depends on the semi-variance at the smallest lag distance. According to the evolution of network design and station density, the time series will present different smallest lags at different times (in a first order approximation all datasets share a decrease of lag distance over time). Therefore one cannot exclude a lack of homogeneity of the extrapolated nugget variance according to the smallest lag distance. However, even though these effects can influence the accuracy of the individual estimates, they are not supposed to result in a systematic bias towards higher or lower values.

5 Summary and conclusions

Temporal variations in the spatial autocorrelation structure of air quality data can reflect changes in the performance and operational conditions of a monitoring network (improvement or worsening of the measurement uncertainty, increase/decrease of the number of monitoring stations, positioning of stations, and shifting in the station classification). However, these phenomena are interfering with changes of the spatial distribution of air pollutants due to transport, emissions and reactions.

In this exploratory study we investigated time series of variogram parameters by applying the Kolmogorov-Zurbenko filtering method. Furthermore, the significance of long term trend components was investigated by a block-bootstrap-based approach combined with linear regression. A significant trend component was found in the nugget time series of France (decrease) and Great Britain (slight increase), and in the range time series of France and Germany (both increasing). Furthermore, a pronounced cyclic behaviour of the seasonal time series component was detected. This seasonal effect is associated with a phase relationship (winter increase) of the nugget and of the partial sill series for several countries, which is particularly pronounced for Austria and Italy. Such effects are likely attributable to limitations in spatial continuity (stronger topographic roughness and dissection of these two countries).

The results obtained so far are promising. In fact, the method can provide indicators of measurement uncertainty trends and changes in the homogeneity/heterogeneity of the spatial distribution of air pollutants. However, further investigations are needed to better determine if the observed trends and variations are caused by changes in the performance

of the monitoring activities, or by seasonal and long term variations of air pollution and/or meteorological factors. For future work, it should be aimed to further improve the robustness of the variogram fitting procedures and to thereby obtain more complete and gap-free time series for the trend analysis. We currently limited the assessment to the data available from AirBase v.4 for the ten years time frame of 1997 to 2007. Prospective future work could profit from the advantages of using an updated version of AirBase. We anticipate that such an extension of the analysis to a more comprehensive dataset with longer time series would immediately be beneficiary to the expressiveness of the results.

Seen from another point of view, the method can have the potential for being developed into a tool for assessing the spatial representativeness of air quality monitoring stations. Example given, commonly used definitions of spatial representativeness are often based on the similarity of concentrations between monitoring stations. Hence, the representativeness area is defined as the area where the concentrations do not differ from the concentration observed at the station by more than a certain threshold. In this context one could aim to investigate the temporal evolution of the variogram function by extracting time series of lag distances intercepting with a specific semivariance threshold which would be chosen equal to the threshold level of the similarity-based spatial representativeness criterion.

References

- Canty, A. and Ripley, B. (2013) *Boot: Bootstrap R (S-Plus) Functions*, R Package Version 1.3-9 [online] <http://CRAN.R-project.org/package=boot> (accessed June 2014).
- Close, B. and Zurbenko, I.G. (2013) *kza: Kolmogorov-Zurbenko Adaptive Filters*, R Package Version 3.0.0 [online] <http://CRAN.R-project.org/package=kza> (accessed June 2014).
- Davison, A.C. and Hinkley, D.V. (1997) *Bootstrap Methods and their Applications*, Cambridge University Press, Cambridge, ISBN 0-521-57391-2.
- Eskridge, R.E., Ku, J.Y., Rao, S.T., Porter, P.S. and Zurbenko, I.G. (1997) 'Separating different scales of motion in time series of meteorological variables', *Bulletin of the American Meteorological Society*, Vol. 78, pp.1473–1483.
- Gerboles, M. and Reuter, H.I. (2010) *Estimation of the Measurement Uncertainty of Ambient Air Pollution Datasets Using Geostatistical Analysis*, 38pp, JRC Technical Reports 59441, EUR 24475 EN, DOI 10.2788/44902.
- Gerboles, M., Reuter, H.I. and Kracht, O. (2016) 'Feasibility of automatic estimations of measurement uncertainty, detection of abnormal values and check of site classification in large air pollution datasets of AirBase', *Atmospheric Environment*, in preparation.
- Kracht, O., Gerboles, M. and Reuter, H.I. (2014) 'First evaluation of a novel screening tool for outlier detection in large scale ambient air quality datasets', *Int. J. Environment and Pollution*, Vol. 55, Nos. 1/2/3/4, pp.120–128.
- Künsch, H.R. (1989) 'The jackknife and the bootstrap for general stationary observations', *Annals of Statistics*, Vol. 17, No. 3, pp.1217–1241.
- Matheron, G. (1963) 'Principles of geostatistics', *Economic Geology*, Vol. 58, No. 8, pp.1246–1266.
- McLeod, A.I. (2011) *Kendall: Kendall Rank Correlation and Mann-Kendall Trend Test*, R Package Version 2.2 [online] <http://CRAN.R-project.org/package=Kendall> (accessed June 2014).
- Pernigotti, D., Gerboles, M., Belis, C.A. and Thunis, P. (2013) 'Model quality objectives based on measurement uncertainty. Part II: NO₂ and PM₁₀', *Atmospheric Environment*, Vol. 79, pp.869–878.

- R Development Core Team (2014) *R: A Language and Environment for Statistical Computing* [online] <http://www.R-project.org/> (accessed June 2014).
- Rao, S.T., Zurbenko, I.G., Neagu, R., Porter, P.S., Ku, J.Y. and Henry, R.F. (1997) 'Space and time scales in ambient ozone data', *Bulletin of the American Meteorological Society*, Vol. 78, pp.2153–2166.
- Wise, E.K. and Comrie, A.C. (2005) 'Extending the Kolmogorov-Zurbenko filter: application to ozone, particulate matter, and meteorological trends', *Journal of the Air and Waste Management Association*, Vol. 55, No. 8, pp.1208–1216.